Science & Technology Facilities Council

Fast transmittance modelling of the MSG and MTG solar channels for cloud retrievals

Final Report

VERSION 1.1

Prepared by

STFC
Rutherford Appleton Laboratory
Chilton, Didcot OX11 0QX, U.K.

in response to
EUMETSAT RFQ 10/202521

Date: 25 March 2011

Contents

1 Introduction....5
2 Task 1: Narrow-band channels....5
2.1 Introduction....5
2.2 Prediction of transmission in RTTOV....6
2.3 Line-by-line Calculations....7
2.4 Determination of two-way transmission with RTTOV. 8
2.5 Accuracy of the derived coefficients....12
3 TASK 2: Wide band 3.8μm channels....16
3.1 Introduction....16
3.2 Optical properties 16
3.3 Testing accuracy of the fast model. 17
3.4 Results 19
3.5 RTTOV coefficients for the 3.9μm sub-channels....23
3.6 Effect of assumed liquid cloud size distribution width parameter on simulated radiances 25
4 Summary and conclusions....28
5 References....29
6 Delivered Files....29

Acronyms

AATSR	Advanced Along-track Scanning Radiometer
ATSR	Along-track Scanning Radiometer
AVHRR	Advanced Very High Resolution Radiometer
BRDF	Bi-directional reflectance distribution function (of a reflecting surface)
CM	Cloud-model
COT	Cloud optical thickness
CTP	Cloud-top pressure
FCI	Flexible Combined Imager
FM	Forward model
IASI	Infrared Atmospheric Sounding Interferometer
ISRF	Instrument spectral response function
LBL	Line-by-line
LOS	Line-of-sight
LUT	Look-up-table
LZA	LOS or view zenith angle
MSG	Meteosat Second Generation
MTG	Meteosat Third Generation
OCA	Optimal cloud analysis
OE	Optimal estimation
RFM	Reference Forward Model
RT	Radiative transfer
RTTOV	RT model for the Tiros Operational Vertical sounder.
SEVIRI	Spinning Enhanced Visible InfraRed Imager
SZA	Solar zenith angle
TOA	Top-of-atmosphere

1 Introduction

The following report describes work carried out in response to Eumetsat RFQ No. 10/202521 07/840 “Fast transmittance modelling of the MSG and MTG solar channels for cloud retrievals". The work builds on that carried out in the study "Cloud Model for Operational Retrievals from MSG SEVIRI” (EUM/CO/07/4600000463/PDW), hereafter referred to as the CM study. The new work has developed fast methods for modelling radiances in the MSG-SEVIRI and MTG-FCI channels, suitable for use in the Eumetsat Optimal Cloud Analysis (OCA) retrieval scheme.

The planned work was divided into two tasks:

1. Consolidate the approach developed in the Cloud-Model (CM) study to the SEVIRI narrow band channels and extend it to the anticipated MTG FCI narrow band channels.
2. Devise a method to accurately model the SEVIRI 3.9 μm channel and the MTG FCI equivalent(s).

Deliverables of the project are:

- This report which details the methods used and accuracy of the transmission model.
- A database of line-by-line (LBL) calculated transmissions (monochromatic and channel convolved)
- "Offline" IDL code used to generate the coefficients for RTTOV from the LBL database.
- The generated RTTOV format coefficient files
- Software documentation consisting of a working description of the delivered s/w at sufficient level of detail to enable knowledgeable users to operate the system

2 Task 1: Narrow-band channels

2.1 Introduction

In the CM study clear-sky transmission in the SEVIRI solar channels was simulated by an approach based on that of RTTOV (rather than the standard OCA method of using tabulated transmission computed using LOWTRAN for certain fixed conditions).

In the time since this work was carried out, RAL has developed a capability to derive coefficients for use with the RTTOV-9[1] code, based on line-by-line (LBL) calculations performed by the Oxford RFM model. The capability was originally developed to allow new spectroscopic data to be used to improve the coefficients used in IASI ozone retrievals. The tools have since been used to allow modelling of additional species with RTTOV e.g. HDO in IASI spectra and SO_2 in HIRS channels. Coefficients derived using the RAL code are written in the standard RTTOV format and so the standard RTTOV code can be used without modification to perform calculations with the new coefficients.

[1] For further details on the RTTOV-9 and the coefficients used by it refer to Matricardi 2008, ECMWF Memo 564, http://www.ecmwf.int/publications/library/ecpublications/_pdf/tm/501-600/tm564.pdf.

Here we use this new capability to generate RTTOV coefficients for all MSG-SEVIRI and MTG-FCI channels with centre wavelength in the range 0.4-4µm (including HRV channels). The code has been extended within this study to output coefficients in RTTOV7 format, similar to the standard coefficient files for the SEVIRI thermal channels. In addition coefficients for the 4 sub-channels derived in task 2 for better modelling of the 3.9µm channel have been derived. Furthermore, coefficients for the solar channels of the following additional instruments have been generated (this work goes beyond the SOW): ERS-2 ATSR2, Envisat AATSR, Metop AVHRR, Aqua MODIS.

2.2 Prediction of transmission in RTTOV

As described in e.g. [Matricardi, 2008], RTTOV performs rapid calculations of radiances for various thermal infra-red sounders and imagers. A fundamental step is the calculation of spectral-response-function convolved, clear-sky atmospheric transmissions from space to a fixed set of pressure levels. In the case of RTTOV7 coefficients for SEVIRI, there are 43 levels spanning 0.1 to 1013.25 hPa and transmissions are considered to be functions of channel, viewing geometry, temperature, pressure, water vapour and ozone. Other significant trace-gases are included in the prediction but are considered to have fixed profiles. The prediction of channel spectral-response-function convolved transmission from space to level *j* is carried out as follows:

$$t_j = \exp(- \tau_j)$$

Equation 1

Where the effective optical depth from space to level *j* is calculated by summing contributions from water vapour, ozone and all other ("mixed") gases:

$$\tau_{0:j} = \tau_{0:j,mixed} + \tau_{0:j,H2O} + \tau_{0:j,O3}$$

Equation 2

Each layer to space optical depth is obtained by summing effective individual layer optical depths:

$$\tau_{0:j,gas} = \sum_{k=1,j} \tau_{k,gas}$$

Equation 3

Where

$$\tau_{k,gas} = \sum_{l=1,Np,gas} c_{l,gas} p_{l,gas}$$

Equation 4

Here $p_{l,gas}$ is a *predictor*, a defined (channel independent) function of the variable parameters (water vapour, temperature etc), and $c_{l,gas}$ are (channel dependent) fixed coefficients for each channel and atmospheric layer. The coefficients are determined by performing a regression of the predictors against a set of explicit line-by-line (LBL) calculations of layer to space transmission for a wide range of atmospheric and viewing conditions. These line-by-line calculations are computationally expensive as they must be first performed at monochromatic resolution (typically requiring many thousands of spectral points per instrument channel) before being convolved with the relevant instrument spectral response.

We refer to *effective* optical depth since these are the layer optical depths which are expected to give the correct spectral-response-function convolved layer to space transmission after applying equation 1 (not e.g. the spectral-response function convolved optical depth or transmission for the individual layer).

The coefficients for predictors associated with mixed gases, ozone and water vapour are determined by separate fits to individual gas effective transmissions derived from the line-by-line calculations as follows:

$$\tau'_{0:j,O3} = \ln(t'_{0:j,xO3}) - \ln(t'_{0:j,all})$$

Equation 5

$$\tau'_{0:j,H2O} = \ln(t'_{0:j,xO3xH2O}) - \ln(t'_{0:j,xO3})$$

Equation 6

$$\tau'_{0:j,mixed} = -\ln(t'_{0:j,xO3})$$

Equation 7

Where

- $t'_{0:j,all}$ is the LBL calculation of the transmission from space to level *j* including all gases
- $t'_{0:j,xO3}$ is the corresponding transmission but excluding ozone from the atmosphere
- $t'_{0:j,xO3xH2O}$ is the result when both ozone and water vapour are excluded.

Note that

$$t'_{0:j,all} = \exp\left(-\left(\tau'_{0:j,mixed} + \tau'_{0:j,H2O} + \tau'_{0:j,O3}\right)\right)$$

Equation 8

I.e. correctly predicting the individual gas optical depths, gives the correct total transmission.

True layer optical depths are given for each gas by

$$\tau'_{k,gas} = \tau'_{0:k,gas} - \tau'_{0:k-1,gas}$$

Equation 9

LBL calculations are perform for n_{atm} different atmospheric states (describing co-varying profiles of temperature, pressure, water vapour, ozone and other gases) and n_{zen} view geometries. At each layer one has n_{atm} times n_{zen} different values of $\tau'_{k:gas}$ Since the atmospheric state is known, the values of the predictors associated with each of these results is known. Standard least squares fitting code can then used to determine the $N_{p,gas}$ unknown coefficient values which give the best match of the predicted $\tau'_{k,gas}$ to the LBL derived "true" $\tau'_{k,gas}$. In the case of the standard RTTOV 7 coefficients which are used here to model MSG SEVIRI transmissions, there are 10 predictors for mixed gases, 15 predictors for water vapour and 11 predictors for ozone.

2.3 Line-by-line Calculations

In the study here we use the MIPAS reference forward model (RFM, see http://www.atm.ox.ac.uk/RFM/) to perform the transmission calculations which are used

as a basis for the calculation of coefficients. Details of the calculations are itemised below.

1. Calculations are performed for the 83 atmospheric profiles defined in [Matricardi, 2008] which are supposed to span the realistic range of conditions likely to be encountered globally. These contain realistically co-varying water vapour, ozone, temperature and pressure profiles. This set of profiles is used to derive the RTTOV coefficients and is referred to as the "training profile set"
2. Calculations are also performed for 83 profiles randomly sampled geographically from a day of ECMWF analysis data (13 June 2008). These results are used to verify the performance of the coefficients and are referred to as the "independent profile set".
3. RFM is run in plane parallel mode to calculate transmissions for view zenith angles of 0, 10, 30, 50, 60, 70, 80^o (for each of the 83 profiles). (The 10^o case is not important, other angles are chosen to be approximately evenly spaced in the secant of the zenith angle).
4. Calculations include the following species H_2O, CO, CO_2 CH_4 HNO_3 SO_2 NH_3 O_2, F11 F12 F14 F22 and SF_6. Note that O_3 is not included in the atmosphere at this stage (since there is no significant line spectra in the range), see point 9 below.
5. Hitran 2008 line data is used.
6. For the training profiles, RFM is also run without H_2O in the model atmosphere.
7. Calculations are performed at monochromatic resolution from 2300 to 19000 cm^{-1}, with some gaps (below 7000 cm^{-1}) where there is no sensitivity from any channel of the instruments listed above.
8. These transmissions are initially convolved with the IASI spectral response function (approximately a 0.5cm^{-1} wide Gaussian function) and then sampled onto a 0.25 cm^{-1} regularly spaced wavenumber grid. These results are stored and used as the basis for all further work (monochromatic results are not stored to avoid unnecessarily large storage requirements).
9. Line by line-transmissions are multiplied by the ozone transmission predicted based on cross-section data provided with the GOMETRAN radiative transfer model (from Bass & Johnsten, 1975) before convolution with the instrument spectral response function. As a consequence of this approach, the data files containing the 0.25cm^{-1} sampled transmission do not contain ozone absorption, but the instrument channel specific files do.
10. The transmissions are convolved with the appropriate spectral response functions for each instrument / channel. These results stored and form the basic input to the regression. For SEVIRI these functions were obtained from EUM/MSG/TEN/06/0010. For MTG, approximate functions were constructed for this study by P. Watts.
11. For the training set, channel convolved transmissions are computed with all gases, all gases except O_3 and all gases except O_3 and H_2O.

2.4 Determination of two-way transmission with RTTOV.

RTTOV is designed for calculation thermal IR radiative transfer for near-nadir viewing geometry defined by a single view zenith angle, θ. For the solar radiative transfer with OCA the most important quantity to be determined is the two-way transmission, t_2, from space to the cloud top, along the path defined by solar zenith angle θ_0 and back up to the satellite, along the path defined by the view zenith angle. In the monochromatic case the two-way transmission is equal to the product of the transmission along the individual paths $t_1(\theta_0)$ and $t_1(\theta)$, i.e. $t_2(\theta_0,\theta) = t_1(\theta_0)t_1(\theta)$. However, this is not generally true for

channel-response function convolved transmissions. If the atmosphere is assumed to be plane parallel, then the two way transmission is equal to the one-way transmission for an effective zenith angle:

$t_2(\theta_0,\theta) = t(\theta')$

Equation 10

Where

$\sec(\theta') = \sec(\theta_0) + \sec(\theta)$

Equation 11

Figure 1 illustrates the variation of θ' with θ_0 and θ.

Using this approximation RTTOV code can be used without modification to compute 2-way transmissions (by computing the single-path transmission for the effective zenith angle θ'). The accuracy of the two-way transmission predicted in this way is limited by the accuracy of the plane-parallel assumption. In the real (spherical) atmosphere the view and solar zenith vary with altitude, and this variation cannot be represented by a single effective zenith angle. However in practise, provided zenith angles are defined at the ground, errors are only significant for OCA if (a) the zenith angles involved are large and (b) there is significant absorption at high altitude (so channels dominated by water absorption are negligibly affected except at (2-way path equivalent) zenith angles larger than 80^o). Errors due to the plane-parallel approximation, for typical atmospheric conditions, are shown in Figure 2.

In the work carried out here we have produced coefficients which cause RTTOV to model the plane-parallel transmission for a given zenith angle[2], so that the model is suitable for computation of two-way transmissions by using the effective zenith angle, but limited by the plane-parallel assumption at high view/solar zenith.

It is noted that it would be reasonably straightforward to improve results for high solar/view zenith by modifying the RTTOV code to accept both solar and view zenith angles and then compute the correct altitude dependent effective path length for each layer, however this has not been done in this study.

[2] Note the coefficients are derived in such a way that RTTOV will generate plane-parallel transmissions despite internally modelling the effect of spherical geometry on the zenith angle appropriate to each layer. This is accomplished by appropriately adjusting the effective angle assumed for each layer in the coefficient regression.

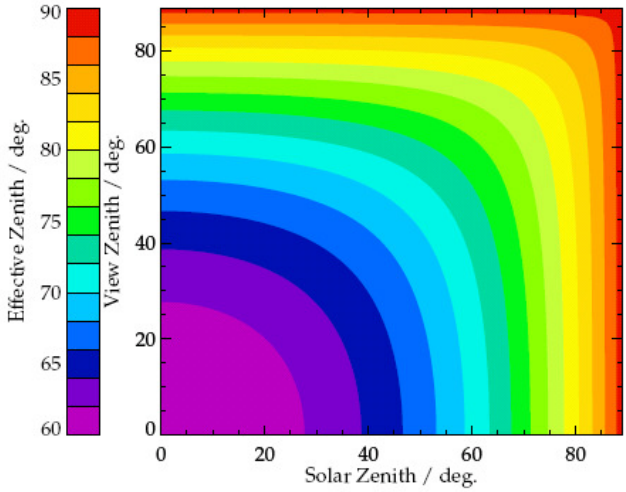

Figure 1: Variation of the effective zenith angle for a 2-way path..

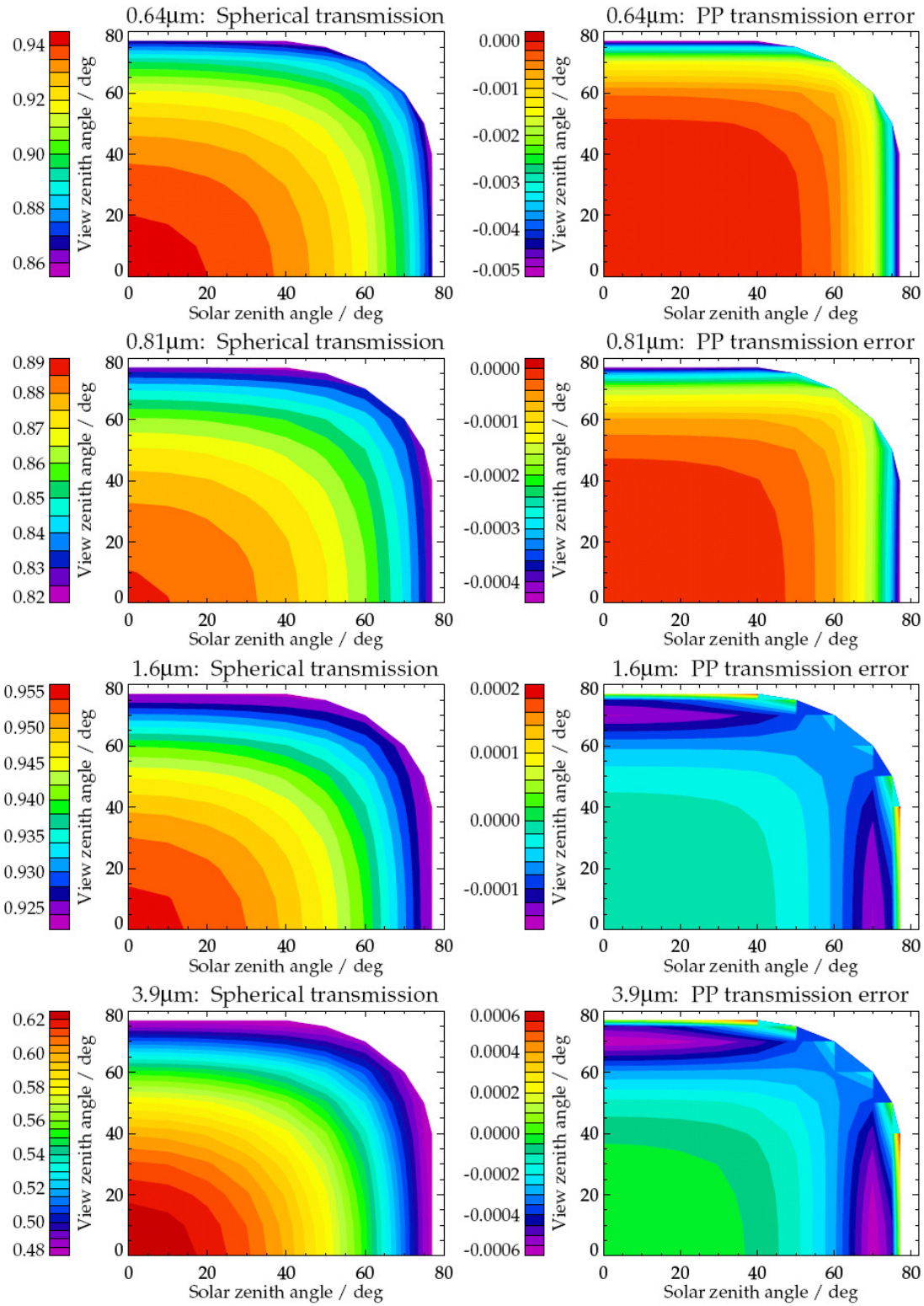

Figure 2: Two-way transmission to the ground in all MSG SEVIRI solar channels (top to bottom), computed with full spherical geometry (left hand column). The right-hand column shows the error in the transmission computed using plane-parallel geometry. Atmospheric conditions are the mean profile from the 83 profile training set.

2.5 Accuracy of the derived coefficients.

Accuracy of the model is assessed by comparing transmission computed using the new coefficients to RFM calculations from the independent profile set. Results are shown in Figure 3 to Figure 5 for MSG-1 SEVIRI, MSG-2 SEVIRI and MTG-FCI, respectively.

Each Figure shows the following:

- Each panel shows results for all instrument channels, each with a different coloured line. For SEVIRI, results are shown for the 0.64-3.9μm main channels, the HRV channel (labelled as 0.71 μm) and the four sub-channels with nominal wavelength from 3.7-4.2 μm which have been derived in task 2 (see below).
- From left to right, panels show the following:
    - The mean "true" transmission (determined by RFM), over all 83 profiles considered, from space to the pressure level indicated on the y-axis.
    - The corresponding standard deviation in the RFM transmission considering all 83 profiles
    - The mean error (bias) between the RFM transmission and that computed using the new coefficients (expressed as % transmission). Note that this is an absolute difference, not the relative difference.
    - The standard deviation in the difference between the RFM transmission and that obtained from the new coefficients.
- From top to bottom, each figure shows results for zenith angles of 30 ^{o} (a single path transmission), 60 ^{o} (corresponding to a two-way path for 0^{o} view and solar zenith) and 80 ^{o} degrees.

It is noted that

- Errors for the SEVIRI channels are always under 1% (except one of the 3.9 micron sub-channels which has a very slightly higher bias near the ground)
- Results for MSG1 and 2 are almost identical
- Results for MTG-FCI are of similar quality to those of SEVIRI, except for the 0.9 and 1.4 micron channels which have slightly larger errors (presumably owing to the larger absorption in these channels).

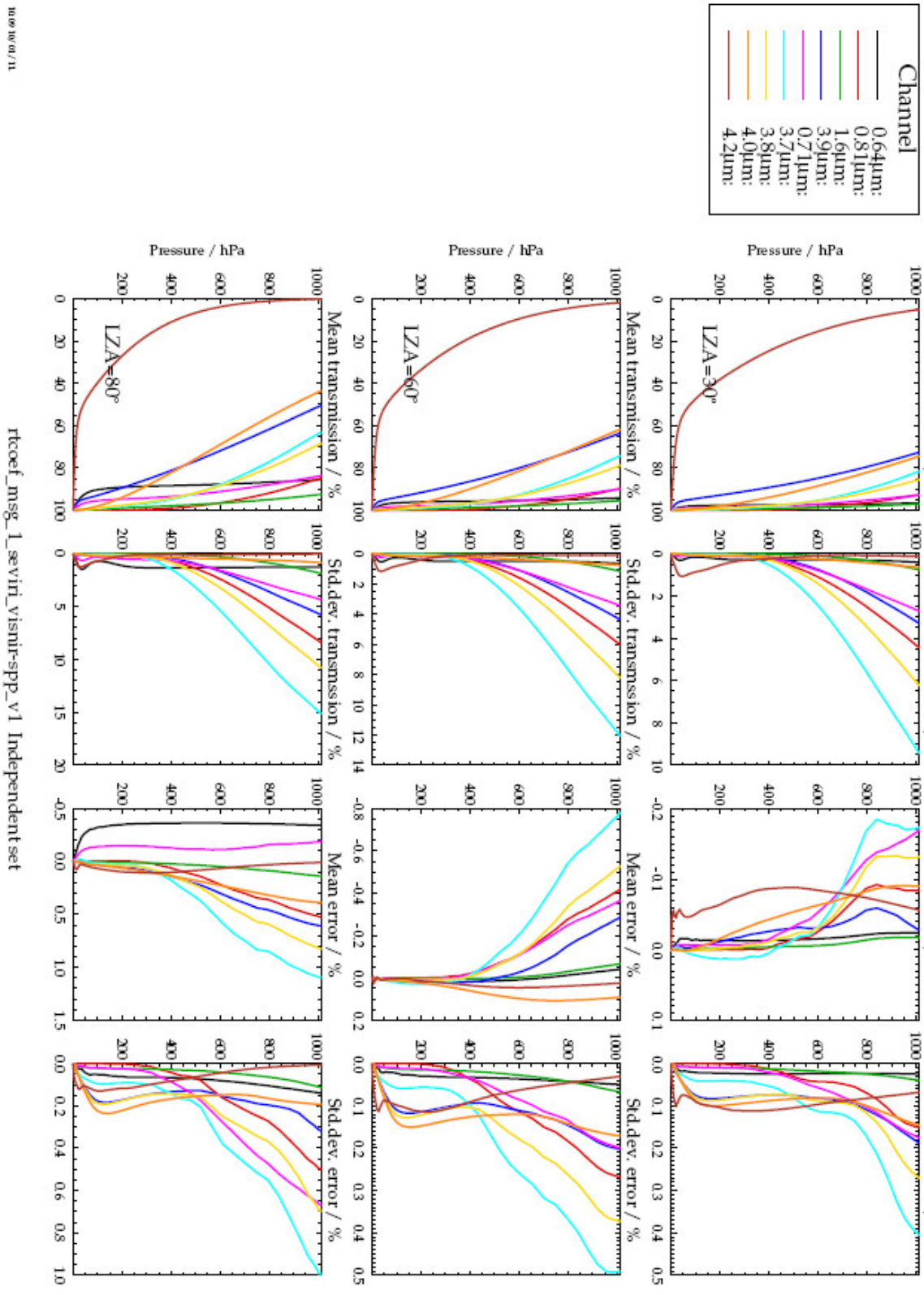

Figure 3: Performance of new coefficients for MSG-1 SEVIRI solar channels.

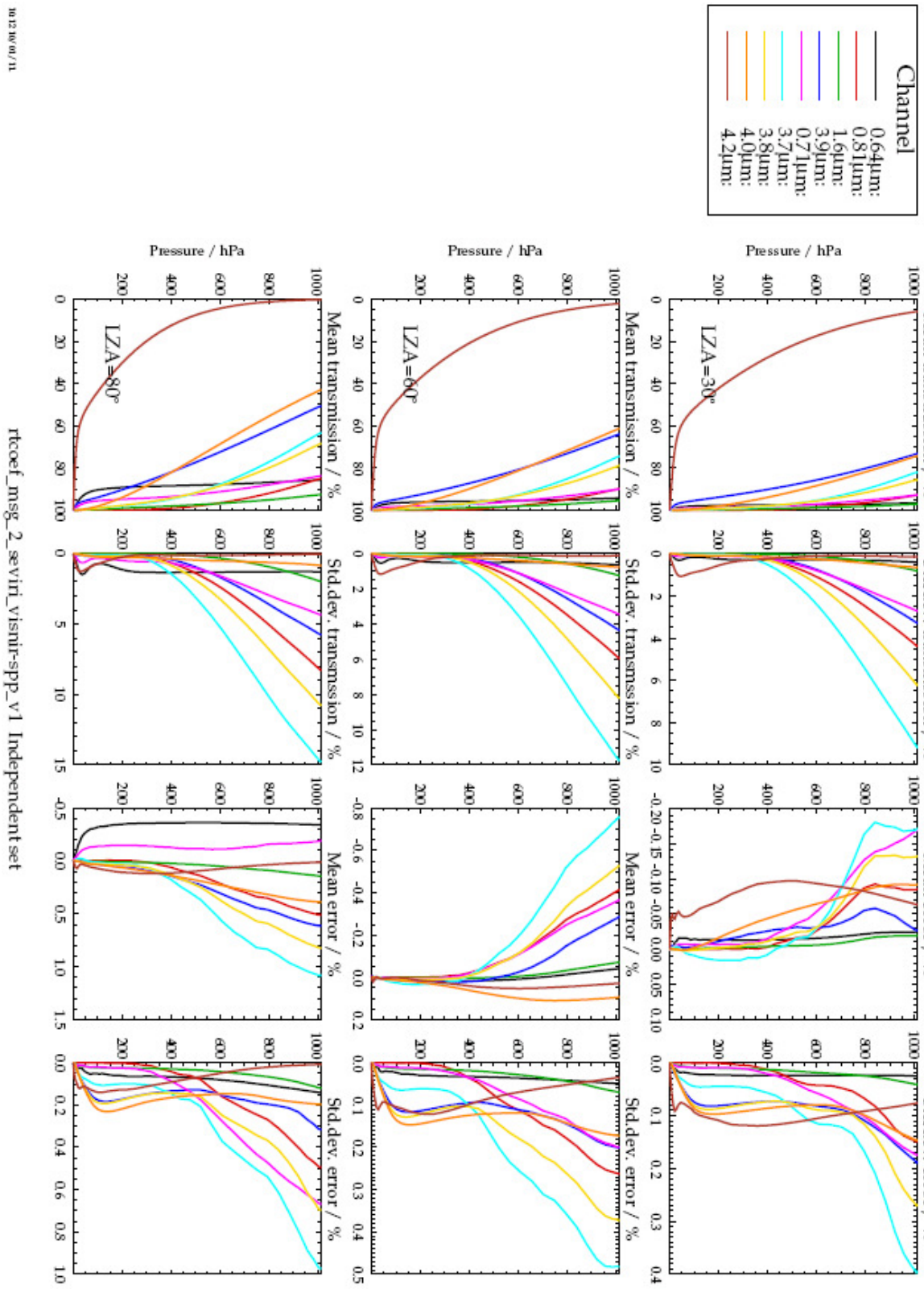

Figure 4: Performance of new coefficients for MSG-2 SEVIRI solar channels.

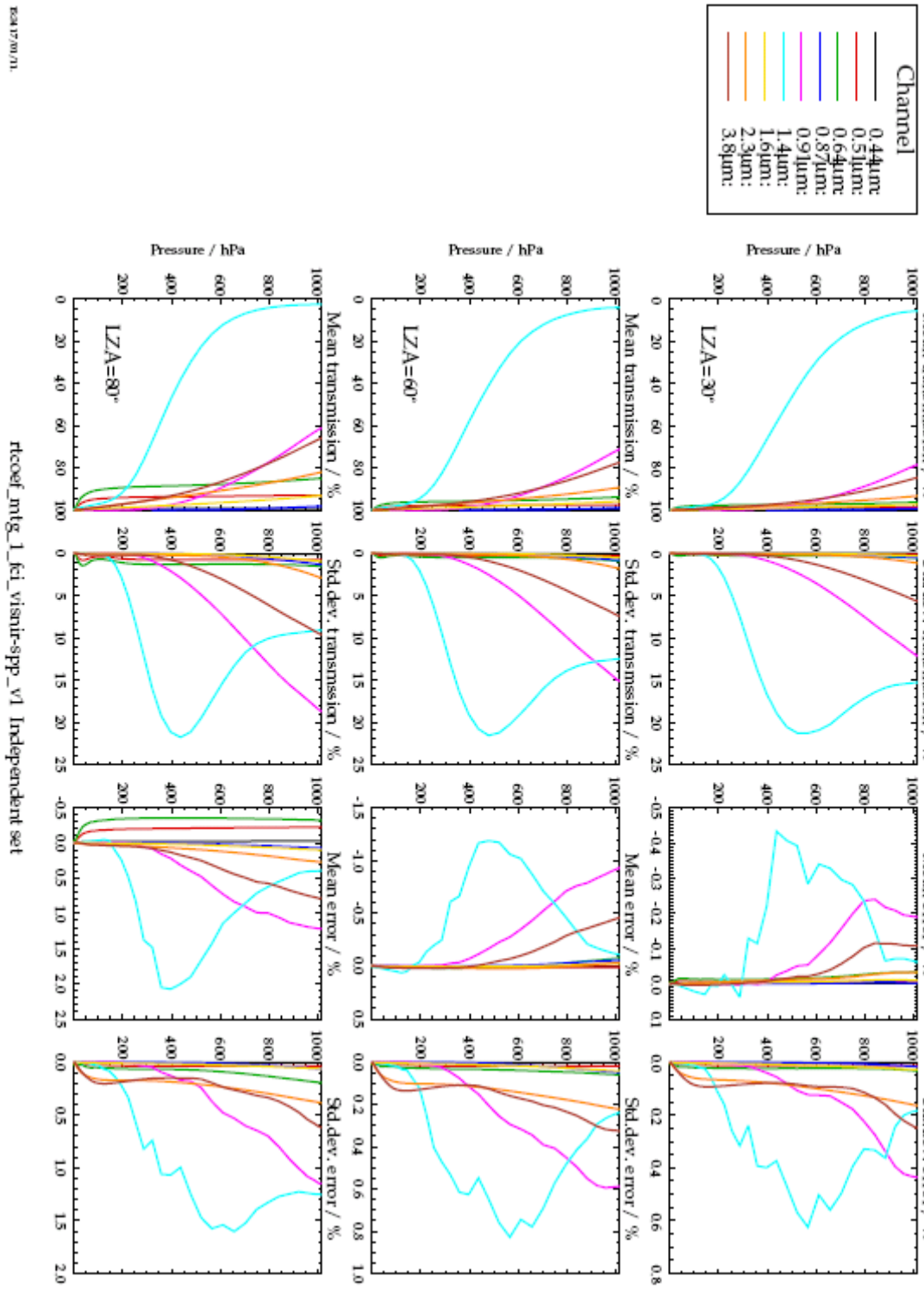

Figure 5: Performance of new coefficients for MTG solar channels.

3 TASK 2: Wide band 3.8µm channels

3.1 Introduction

The CM-study and parallel work at Eumetsat has demonstrated that the 3.9µm channels can be difficult to fit in retrievals. It has been recognised that the 3.9µm spectral-response function is broad and covers a region in which a number of optical parameters, such as trace-gas transmission, cloud reflectance and surface albedo, have large spectral variation. The standard OCA forward model performs effectively monochromatic radiative transfer using spectrally averaged values for these optical properties. Here we investigate whether this quasi-monochromatic approach can lead to inaccuracy in radiative transfer sufficient to explain the discrepancies found in real retrievals.

In the case that the quasi-monotonic assumption leads to significant error, it is clear that the model could be made sufficiently accurate by performing standard-OCA forward calculations for a number of narrow-band sub-channels and suitably weighting these to give the broad-band simulated radiance. In this task we seek to define a (small) set of sub-channels which enable a sufficient accuracy to be obtained without undue increase in computational demands.

As noted in the SOW, here "sufficient" is judged in relation to other errors affecting the cloud retrieval. We aim to define sub-channels which give sub 1K BT errors over a wide (but not complete) range of conditions, with the expectation that results would be substantially better under most conditions.

3.2 Optical properties

Here we model spectral variations in the following parameters as follows.

- Solar illumination using the ACE-FTS solar spectrum [Hase,2010]
- Water cloud optical properties. We focus on water cloud effects as the relevant spectral dependence can be simulated with confidence from the known refractive indices. Refractive indices are computed using the REFWAT code from Piotr Flatau. These refractive indices are use in Mie calculations to generate the standard OCA radiative transfer look-up-tables (LUTs) for spectral points spanning the 3.9µm spectral response at 4 cm^{-1} resolution. The LUT parameters are subsequently interpolated to finer spectral sampling as required.
- Surface (land / ocean) reflectivity and emissivity. Here we take some scenarios designed for the ESA Camelot study [Veefkind, 2009]. The reflectivities are shown in Figure 6. Surfaces are assumed to be Lambertian with the albedo shown in the figure and emissivity is assumed to be 1-albedo.
- Clear-sky absorption. This is modelled using RFM calculations preformed in task 1 for the RTTOV coefficient training set.

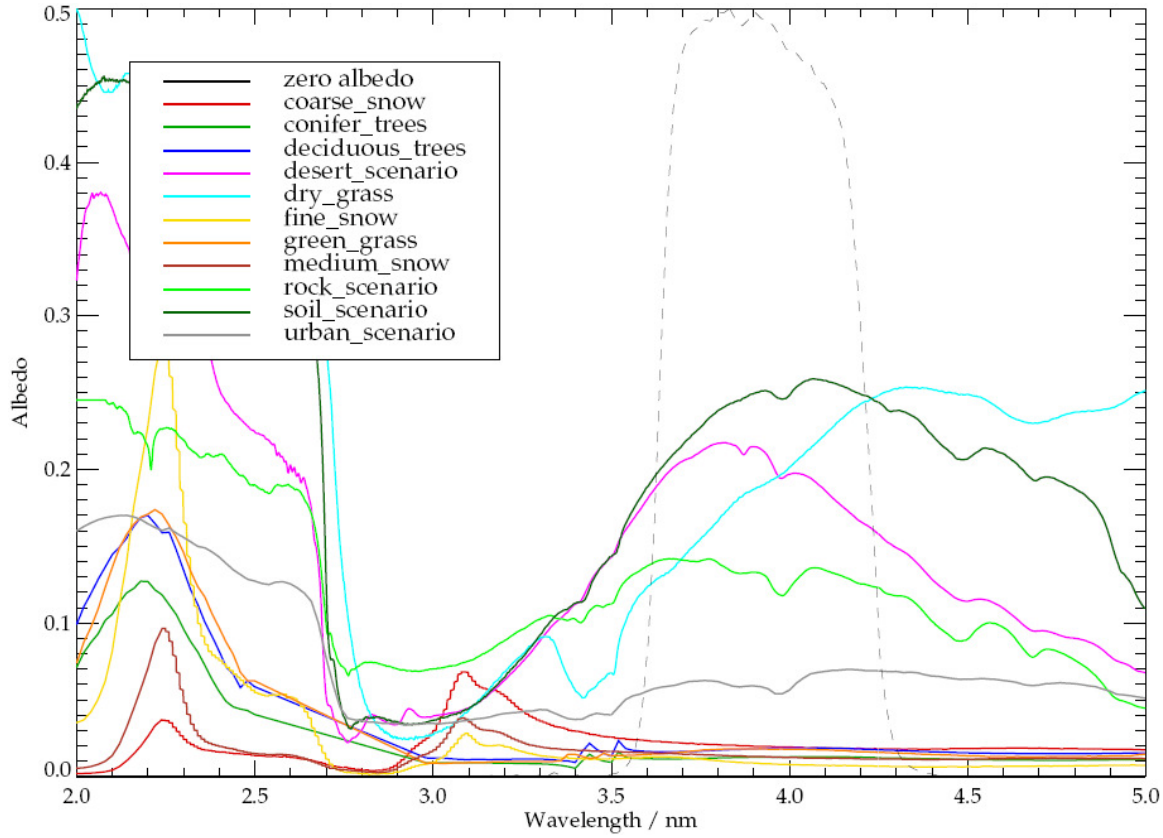

Figure 6: Spectral surface reflectance (assumed equal to Lambertian albedo here) from ESA Camelot study. Dashed line shows the 3.9μm spectral response function.

3.3 Testing accuracy of the fast model.

The accuracy of the OCA approach is tested as follows:

- Optical properties are computed at 0.5cm-1 resolution and 0.25cm-1 sampling across the 3.9μm micron spectral response at "high" spectral resolution.
- Optical properties at this sampling are spectrally averaged to 2cm^{-1} sampling[3].
- The optical properties are obtained at each point on the 2cm^{-1} sampled grid.
- Radiances are computed for each spectral point in the grid using the spectrally resolved optical properties (for one of the 83 training profile sets and computational angles defined previously) and the standard OCA LUT forward model (FM).
- The resulting radiances are convolved with the instrument spectral response function to give the supposed true radiance, R_{true}. R_{true} is the sum of the solar and thermal contributions:

$$R_{true} = R_{true:solar} + R_{true:thermal}$$

Equation 12

These are converted to brightness temperature (BT) to give $B_{true,,}$ $B_{true:solar}$ and $B_{true:thermal}$.

[3] This step is performed to speed-up subsequent calculations and was confirmed to make negligible (<0.1K) difference to channel averaged radiances compared to performing simulations at 0.25cm^{-1} sampling.

- Optical properties are averaged by the spectral response function as follows:
  - Surface reflectance, solar irradiance and the trace-gas transmissions (from space to each level) appropriate for the solar contribution to the signal are each computed by simply convolving the $2cm^{-1}$ sampled values with the spectral response.
  - Note that both above-cloud transmission and total transmission to the surface are modelled with the correct values for the 2-way (solar) path. The transmission from cloud to the surface is inferred from these in the FM, assuming Beer's law (which is not strictly correct). I.e. the transmissions are calculated to correctly model the effect of gas absorption for optically thick cloud and no-cloud. Errors in the fast model can only be introduced by either errors caused by spectral dependence of quantities other than gas absorption or error in modelling gas absorption below cloud when multiple scattering with the surface is important.
  - Trace-gas transmissions for the thermal contribution is derived similarly, but weighting by the Planck function for the level concerned (following the approximation used in RTTOV).
  - LUTs are sampled at the centre-of-mass of the spectral response function (not spectrally averaged).
- The OCA LUT FM is applied to the channel convolved optical properties to give $R_1 = R_{1:solar} + R_{1:thermal}$ and corresponding brightness temperature, B_1.
- The error in the fast FM (in BT) is assumed to be $\Delta B = B_1 - B_{true}$.
- This error is divided into solar and thermal contributions, ΔB_{solar} and $\Delta B_{thermal}$. These quantities are computed by as follows

$$\Delta B_{solar} = f(R_{1:solar} + R_{true:thermal}) - B_{true}$$
$$\Delta B_{themal} = f(R_{true:solar} + R_{1:thermal}) - B_{true}$$

Equation 13

Where f(R) is the function which returns the equivalent BT for radiance R.

The improved accuracy which can be obtained by performing quasi-monochromatic RT for sub-channels is assessed as follows:

- Sub-channel boundaries are defined.
- Each sub-channel, *i,* is assumed to have spectral response defined by the following procedure:
  - Interpolate the 3.9μm channel spectral response onto a $0.25cm^{-1}$ sampled grid. Normalise this function to integrate (over wavelength) to 1.
  - Set values outside the sub-channel boundaries to zero
  - Integrate the function over wavelength to give the relative contribution of the sub-channel to the total channel spectral response. This defines a weight, w_i, which is used later to reconstruct the channel averaged radiance.
  - Re-normalise the sub-channel response by dividing by w_i.
- Optical properties are averaged as above for each of the spectral response functions in turn.
- The OCA LUT FM is applied to obtain radiances, R_i, for each sub channel.
- The estimated channel radiance is obtained from the weighted sum of the sub-channel radiances:

$$R_N = \Sigma_{i=1,N} w_i R_i$$

Equation 14

Not that these tests, by definition, assume the fast FM used by OCA is correct if there are no spectral dependencies in the input parameters. There are many possible additional errors applicable to comparisons of the model and observations, e.g. cloud being of finite vertical thickness, cloud vertical structure, 3D effects, error in microphysical properties and assumed size distribution, error in modelling surface reflection etc. Here we seek to quantify errors only from the quasi-monochromatic assumption.

3.4 Results

Figure 7 illustrates the calculation of channel averaged radiance for a particular case. The top panel shows the spectral dependencies of various quantities affecting the radiative transfer. The vertical lines in the top panel indicate boundaries between 4 sub-channels that have been selected (in ad-hoc fashion) to test the potential for improving the simulation of the channel averaged radiance. The channel boundaries and associated weights are defined in Table 1

The bottom panel in Figure 7 shows the error in simulating the radiance as a function of number of sub-channels. Sub-channel boundaries are based on the 4 sub-channels defined in Table 1 as follows:

- 1 sub-channel refers to the standard approach of calculating channel averaged radiance with a single calculation based on channel averaged optical properties
- 2 sub-channels are defined with boundary at 3.9μm
- 3 sub-channels have boundaries at 3.7 and 4.16μm
- 4 sub-channels are as defined Table 1.
- Multiples of 4 sub-channels are defined by splitting the 4 sub-channels evenly in wavelength.

It is noted that the error even for the single channel calculation is less than 1K. The error can be reduced by using 3 or more sub-channels.

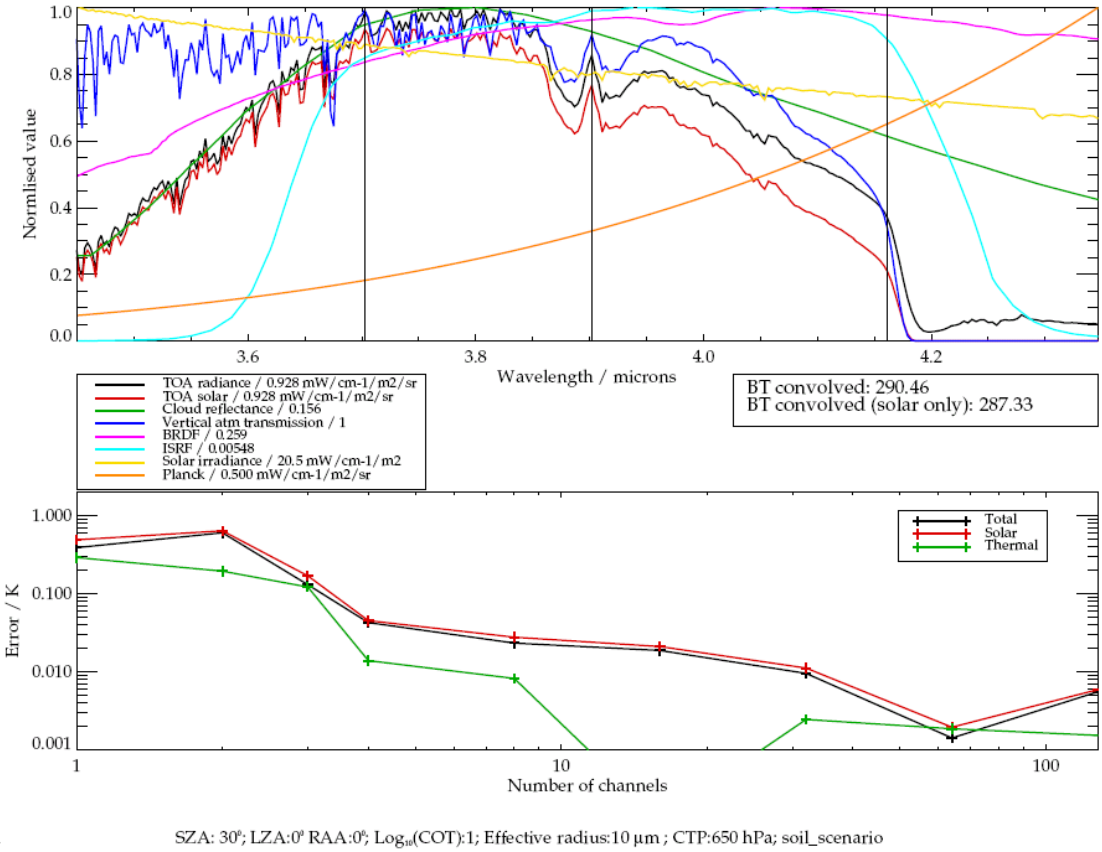

Figure 7: Illustration of the calculation of 3.9µm channel averaged BTs. Top panel shows various terms involved in the calculation of the radiance from 2cm^{-1} resolution optical properties. Each line is normalised for comparison purposes. The value by which each line is normalised is indicated in the caption. The bottom panel shows the BT error in the fast model as a function of the number of sub-channels used. Thermal and solar contributions to the error are shown in green and red, respectively. Cloud and surface conditions for this case are shown in the caption at the bottom of the figure (refer to list of acronyms).

Sub-channel spectral range / μm	Weights	
	MSG1	MSG2
up to 3.7	0.11756	0.13133
3.7-3.9	0.35243	0.33813
3.9-4.16	0.43392	0.44453
above 4.16	0.096082	0.086001

Table 1: Weights to be applied to sub-channel radiance contributions to obtain channel averaged radiance.

Simulations have been conducted for all combinations of the following conditions

- Zenith angle (applied to both solar and view path): 10, 50 and 70°.
- Relative azimuth angle: 20°.
- Cloud-top pressure: 850, 350 and 200 hPa.
- Log_{10} cloud optical depth: -2, -1 ,-0.5 ,0 , 0.5, 1 and 2
- Cloud effective radius: 4, 10 and 20μm.
- Profile number from the 83 profile training set: 80, 81 and 82. These correspond respectively to the minimum, maximum and mean profiles from the set, so span a very wide range of conditions
- Surface types: Zero albedo (indicated by index 0), dry-grass (5) and soil (10).

This results in a large number of results. To visualise the range of errors encountered and diagnose the key parameters which lead to large error, histograms of the BT error for all cases are plotted as function of each of the individual variable parameters above. Results for the single-channel case are shown in Figure 8. Only in a few cases do errors exceed 2K (worst case 2.6K). By examining the histograms, one can see that errors are largest for optical depth of 1 (log10 optical depth 0), bright surface, minimum trace-gas absorption and a high-altitude cloud. In this case errors are presumably related to the modelling of the reflection between cloud and the surface.

Figure 9 shows errors when 4 sub-channels are used. Errors are now reduced to generally less than 1K (worst case 1.5K, again for optical depth 1).

Errors over dark surfaces are less than 1K in the single channel case and less that 0.3K in the 4-channel case.

Errors seen here are not of sufficient magnitude to explain errors seen in practise in fitting the 3.9μm channel (residuals of 5-10K are not uncommon).

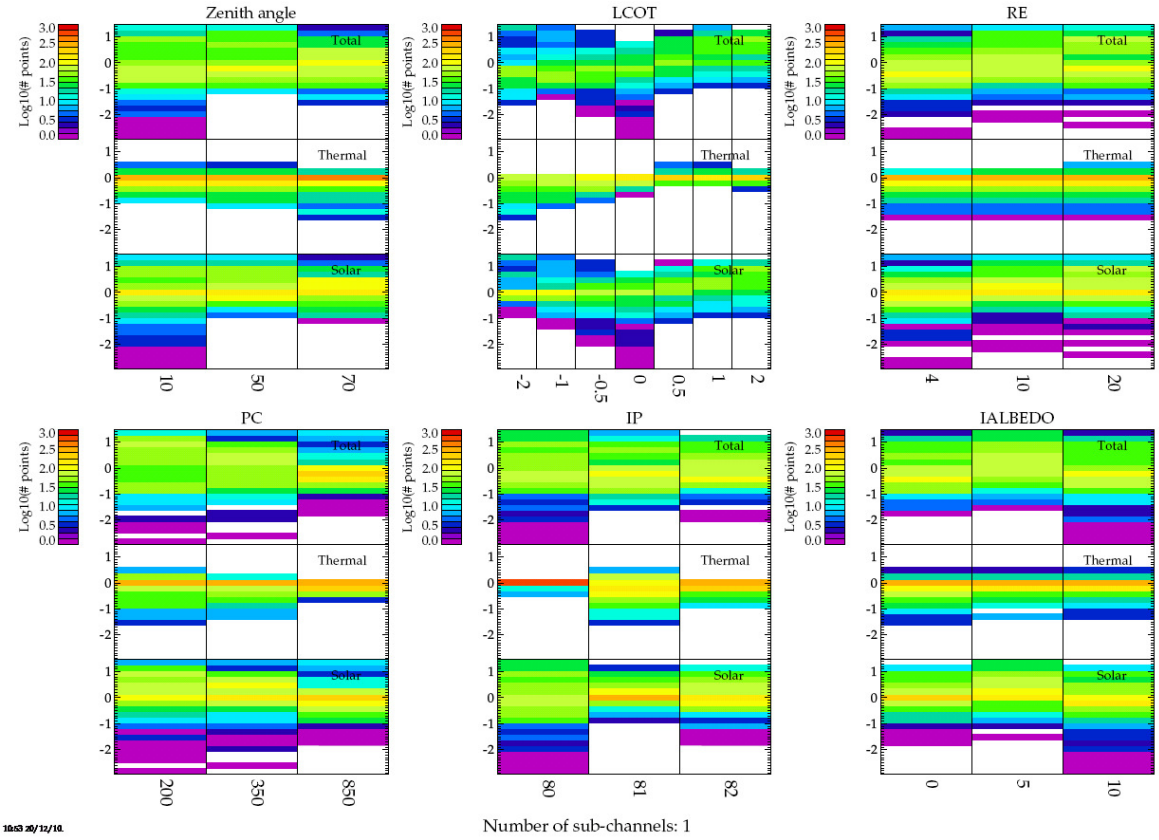

Figure 8: Error in the single-channel FM for the 3.9μm channel as a function of various conditions (see text for details). Each panel shows histograms of the error as a function of a particular parameter (clockwise from top-left: Zenith angle; Log10 cloud optical depth; Effective radius; Cloud-top-pressure, Index of the 83 profile training set; Surface reflectance scenario). Within each panel, 3 histograms are shown corresponding to the total error (top) and the error contribution from thermal (middle) and solar radiation (bottom).

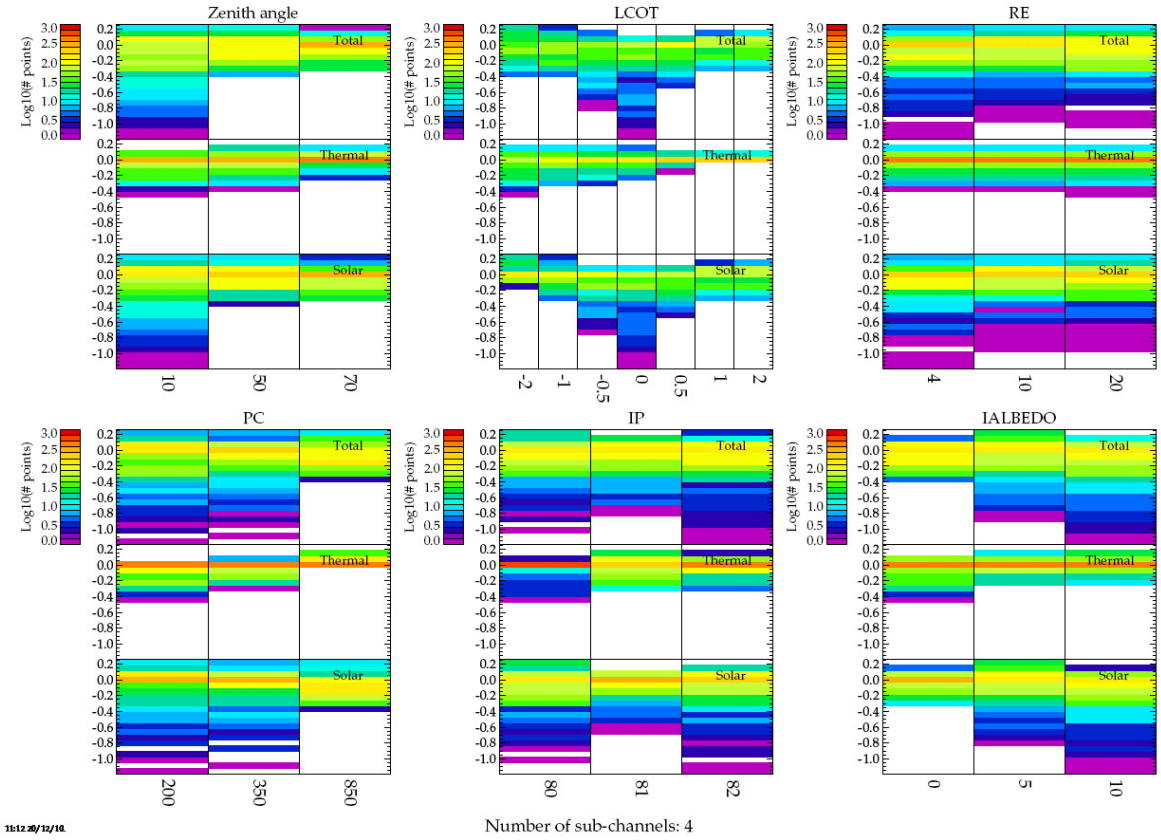

Figure 9: Error in the 4-channel FM for the 3.9μm channel as a function of various conditions (see text for details).

3.5 RTTOV coefficients for the 3.9μm sub-channels

RTTOV coefficients have been generated to enable the 4 sub-channels. The accuracy of these has already been illustrated in Figure 3 and Figure 4 above. In addition, Figure 10 compares transmissions for channel averaged transmission computed by appropriately weighting the individual transmissions for the 4 sub-channels. The accuracy is very similar to that obtained from the new single-channel coefficients (as expected).

Figure 10 also compares transmissions computed by RFM to those obtained from the standard RTTOV coefficients. Results for the 80° case should be disregarded as these coefficients should only be used up to 75°. For other cases the agreement is within 1-2% (bias and standard deviation) which is reasonable and not likely to lead to errors modelling the channel radiance comparable to those found in real retrievals.

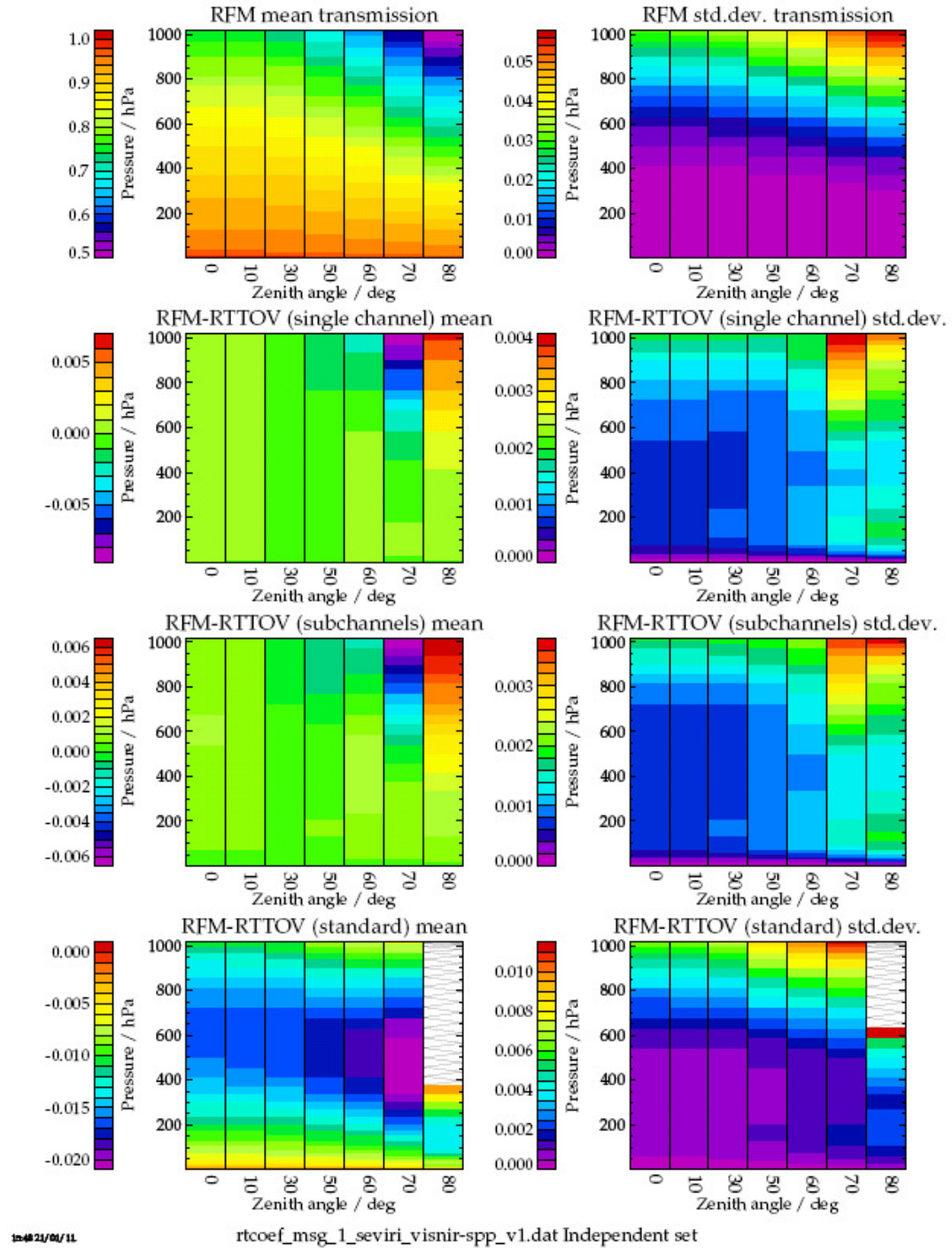

Figure 10: Comparison of 3.9 channel transmissions computed using the coefficients for the selected sub-channels. Top panels show RFM level-to-space transmission and standard deviation (for the independent profile set) as a function of zenith angle and layer pressure. 2nd row shows mean and standard deviation in the difference between the RFM (true) transmission and that predicted by RTTOV using the new single channel coefficients derived in task 1. 3rd row shows the difference between the transmissions computed by taking the weighted sum of the 4 sub-channel transmissions. Bottom row shows the difference between RFM and results from the standard (not Planck-weighted) RTTOV coefficients (i.e. those distributed with the code).

3.6 Effect of assumed liquid cloud size distribution width parameter on simulated radiances

Since errors from the quasi-monochromatic assumption have been found to be quite small compared to residuals encountered in practise, some study effort was diverted from further optimisation of sub-channels into considering other possible sources of the experienced residuals.

The most simple case in which large residuals are encountered is over single-layer stratocumulus cloud over sea. (In more complicated multi-layered scenes inconsistency between the 1.6 and 3.9μm is expected due to the inappropriate nature of the single-layer cloud model.)

For liquid cloud, OCA LUTs are calculated based on Mie calculations, assuming the size distribution to follow a gamma distribution:

$$n(r) = a\, r^{\alpha} \exp(-b.r)$$

Equation 15

Where r is the droplet radius, and a, b, α specify the gamma distribution: The effective radius of the distribution is

$$r_e = (\alpha+3)/b$$

Equation 16

and the effective variance is

$$v_e = 1/(\alpha+3).$$

Equation 17

In OCA the effective radius is a retrieved parameter but α is assumed to be equal to 6.

The sensitivity of radiance simulations to the value of α has been tested by computing LUTs with α=3, 6 and 9 (v_e = 0.17, 0.11, 0.08). Figure 11 shows the relatively modest impact on cloud reflectance for a particular case, as a function of wavelength across the 3.9μm spectral response.

Figure 12 shows how cloud reflectance varies at wavelengths of 0.55, 1.6μm and several wavelengths in the 3.9μm region. Finally, figure 13 shows histograms of the difference between radiances computed assuming α=3 and α=9. Here the following conditions have been assumed:

- Zenith angle (applied to both solar and view path): 10 and 70^o (scattering angles 160.3 and 44.5^o).
- Relative azimuth angle: 20^o.
- Cloud-top pressure: 850 and 200 hPa.
- Log_{10} cloud optical depth: -2, -1 ,-0.5 ,0 , 0.5, 1 and 2
- Cloud effective radius: 4, 8, 10, 12, 14, 16 and 20μm.
- Zero surface albedo

Radiance differences are seen to depend on optical depth and effective radius (much less on cloud height or zenith angle[4]). Errors reach values of around 2K. However one should note that, for effective radii around 10, Figure 12 indicates that the differences at 1.6µm are of comparable magnitude but opposite sign. Hence a retrieval which fits the 1.6µm channel could produce larger errors at 3.9µm than figure 13 might suggest.

Note also that the variation in α simulated here is not particularly large: E.g. Arduini [2005] simulated the effect of v_e varying from 0.1 to 0.3 on GOES cloud retrievals.

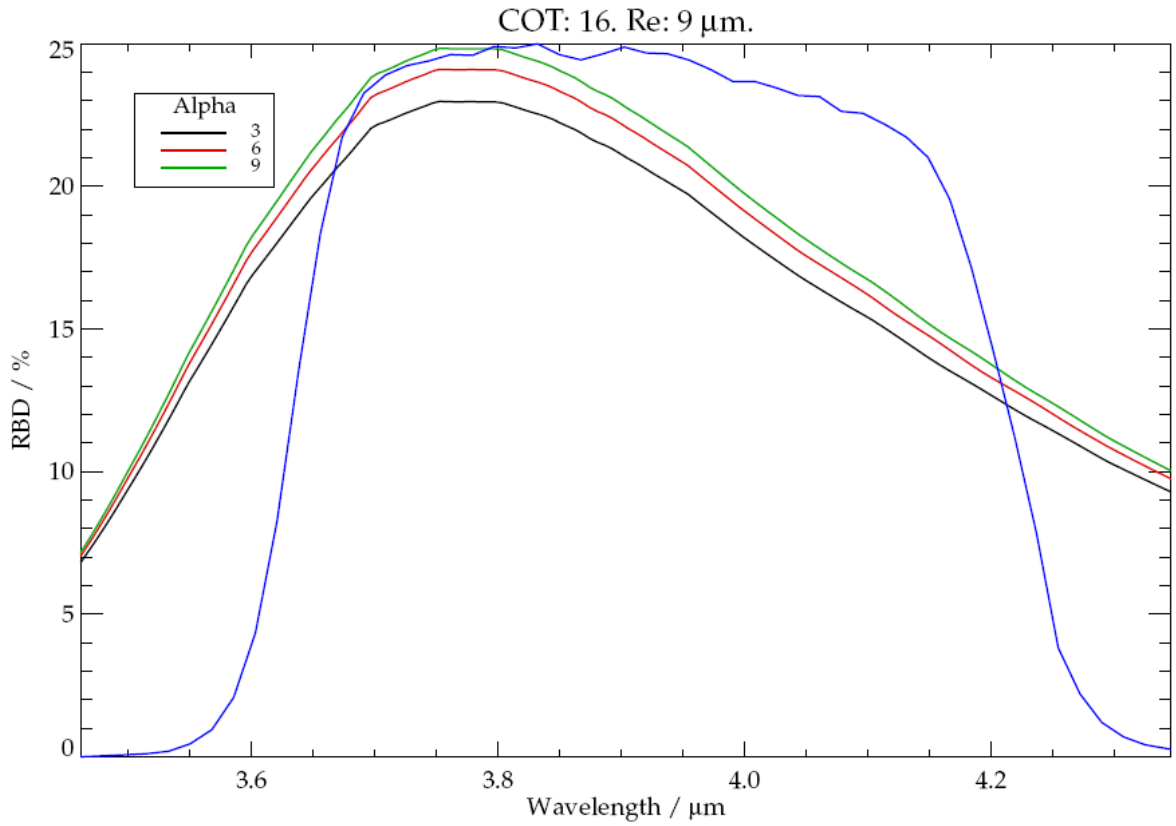

Figure 11: Spectral variation in cloud reflectance (RBD) with size distribution parameter alpha. Blue line shows the 3.9µm spectral response function. Case shown is cloud optical thickness 16 and effective radius 9µm.

[4] It is noted that a complex dependence on scattering angle has been found by other simulations [P.Watts, pri.comm.], however here differences between the two cases are small compared to the effect of varying effective radius and optical depth.

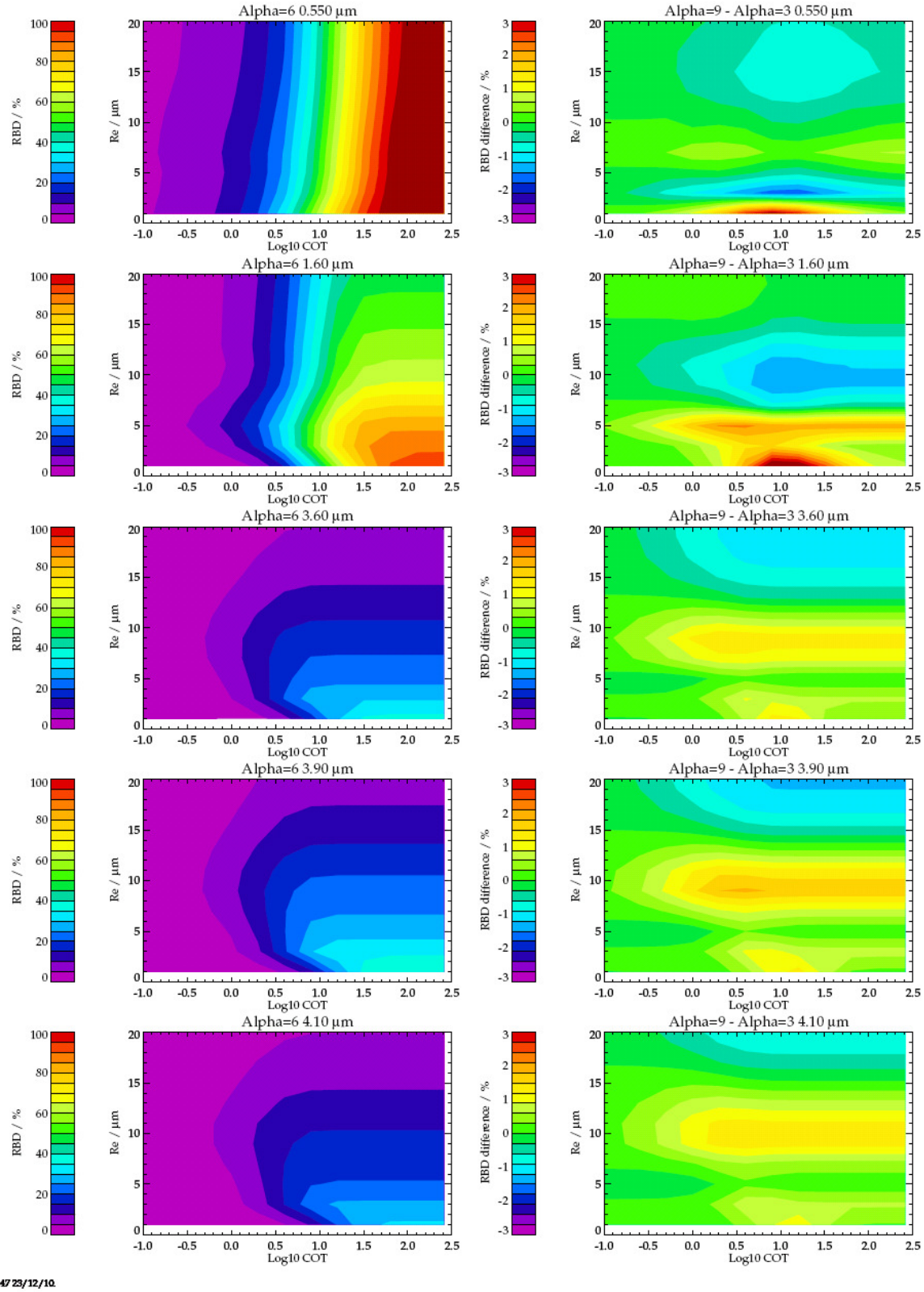

Figure 12: Variation cloud reflectance (RBD) with optical depth, effective radius, and size distribution parameter α. Each row shows results at a different wavelength. All panels are for zero satellite and solar zenith. Panels on the left show RBD for α=6. Blue line shows the 3.9µm spectral response function. Case shown is cloud optical thickness 16 and effective radius 9µm.

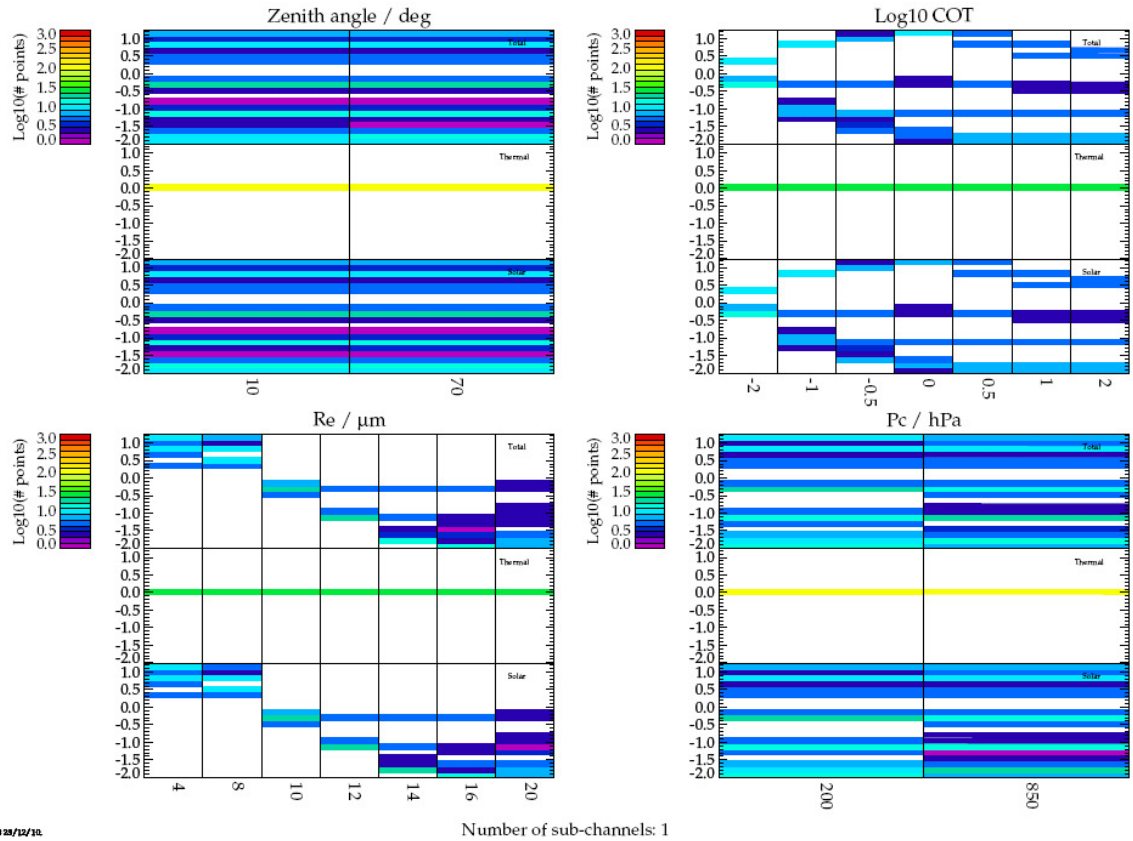

Figure 13: Histograms of the difference in 3.9 µm BTs (K) between calculations which assume α=3 and α=9. Histograms are shown (clockwise from top left) as a function of Zenith angle, log10 cloud optical thickness, cloud-top pressure and cloud effective radius.

4 Summary and conclusions

This study has carried out three specific tasks to refine radiative transfer calculations performed in OCA to simulate SEVIRI radiances:

1. RTTOV coefficient files have been produced which enable RTTOV to simulate 2-way transmission in solar channels rapidly, to an adequate level of accuracy. While the current results meet the requirements of the study, at present the applicability of the results to high view and / or solar zenith is limited by the need to assume plane-parallel geometry. In future it would be desirable to extend RTTOV to accept solar as well as view zenith angle and then enable the 2-way path to be properly computed in spherical geometry. Some investigation of whether accuracy could be improved by refining the predictors or viewing geometries used in training could also be worthwhile.
2. The accuracy of the OCA quasi-monochromatic approach to model the 3.9µm channel has been tested. This has indicated that using channel averaged values of solar irradiance, atmospheric transmission, and cloud and surface reflection / transmission leads to errors of at most a few K, not sufficient to explain larger residuals found when conducting real retrievals. Errors can be reduced to (in almost all circumstances) less than 1K if the OCA quasi-monochromatic approach is applied to 4 sub-channels and the results weighted to give channel averaged radiance.

3. The sensitivity of radiances to the width of the drop size distribution has been tested. Plausible variations in the gamma function width parameter α could produce radiance residuals of a few K at 3.9μm. Given this result, it would seem logical to perform retrieval simulations to further explore this issue. E.g. measurements could be simulated based on field campaign observations of the drop-size distribution, then OCA applied to the simulated radiances and resulting residuals evaluated (as well as errors in optical depth in effective radius).

5 References

Arduini, R.F., Sensitivity of Satellite-Retrieved Cloud Properties to the Effective Variance of Cloud Droplet Size Distribution, Fifteenth ARM Science Team Meeting Proceedings, Daytona Beach, Florida, March 14-18, 2005

Matricardi, M.: Title The generation of RTTOV regression coefficients for IASI and AIRS using a new profile training set and a new line-by-line database Institution ECMWF Year of publication 2008

Frank Hase, Lloyd Wallace, Sean D. McLeod, Jeremy J. Harrison and Peter F. Bernath, The ACE-FTS atlas of the infrared solar spectrum, Journal of Quantitative Spectroscopy and Radiative Transfer, Volume 111, Issue 4, March 2010, Pages 521-528

Veefkind, J.P (ed) CAMELOT Final Report, ESA Contract 21533/07/NL/HE, RP-CAM-KNMI-050 Issue 1, 30 November 2009

6 Delivered Files

New coefficient files can be found at

ftp://ftp.rsg.rl.ac.uk/cloud-model/fasttrans/

The code used to perform the RTTOV coefficient regression has been provided to the agency.

Code is written in the IDL language with some libraries to perform basic functions.

It should be possible to run the code as follows:

- Make a directory for the code and data files e.g. ~/cloud-model.
- Set environment variable CLDMODEL_PATH to this directory.
- Set LD_LIBRARY_PATH to point to $CLDMODEL_PATH/libs
- Obtain all tar files from
  ftp://ftp.rsg.rl.ac.uk:/cloud-model/
- Untar these into directory CLDMODEL_PATH
- Obtain the RFM simulation results from
  ftp://ftp.rsg.rl.ac.uk:/cloud-model/rfm-sims/
- Untar these int $CLDMODEL_PATH/rfm_sims/
  - Open IDL in 32 bit mode (call with -32 flag) and type "*rerun_all_visnir"* at the IDL prompt.

rerun_all_visnir.pro is a main routine which runs all steps of the coefficient regression from RFM 0.25cm^{-1} sampled output files, to the generation of the verification plots included in this report. By default it will read RFM files which have been convolved with instrument spectral response function, however these can be re-created from scratch by setting keyword RFM. Note however that these convolutions are quite time consuming (order days for all instruments).

The main routines call by *rerun_all_visnir.pro* are as follows:

- *rfm2imager*: Code to generate instrument-response function convolved transmissions from the 0.25cm^{-1} sampled “monochromatic” spectra.

- *regress_rttov_rfm*: Generate RTTOV coefficients.

- *test_rtcoef_visnir*: Generate diagnostic plots comparing results from the new coefficients and the original RFM transmissions

- *test_rtcoef_visnir39*: Test 3.9µm transmissions computed from the 4 sub-channels.

For further details, refer to comments in the code.